AIP Journal of Applied Physics

Electric-field effects of dielectric and optical properties in $Pb(Mg_{1/3}Nb_{2/3})_{0.65}Ti_{0.35}O_3$ crystal

Chi-Shun Tu, F.-T. Wang, R. R. Chien, V. Hugo Schmidt, and George F. Tuthill

Citation: Journal of Applied Physics **97**, 064112 (2005); doi: 10.1063/1.1862314
View online: http://dx.doi.org/10.1063/1.1862314
View Table of Contents: http://scitation.aip.org/content/aip/journal/jap/97/6?ver=pdfcov
Published by the AIP Publishing

JOURNAL OF APPLIED PHYSICS 97, 064112 (2005)

Electric-field effects of dielectric and optical properties in $Pb(Mg_{1/3}Nb_{2/3})_{0.65}Ti_{0.35}O_3$ crystal

Chi-Shun Tu[a] and F.-T. Wang
Graduate Institute of Applied Science and Engineering, Fu Jen University, Taipei 242, Taiwan

R. R. Chien, V. Hugo Schmidt, and George F. Tuthill
Department of Physics, Montana State University, Bozeman, Montana 59717

(Received 20 September 2004; accepted 12 December 2004; published online 14 March 2005)

Dielectric properties and domain structure have been measured as functions of temperature in a (001)-oriented $Pb(Mg_{1/3}Nb_{2/3})_{0.65}Ti_{0.35}O_3$ (PMNT35%) single crystal with and without a prior dc electric (E)-field poling. Without E-field poling, the dielectric loss exhibits a frequency-dependent maximum in the region of 120–180 K, which can be described by a Vogel–Fulcher equation and fractal cluster model which implies structural irregularities within domains. With a prior poling a long-range monoclinic (tetragonal)→tetragonal (monoclinic) transition takes place near 212 K upon heating. "Monoclinic (tetragonal)" represents that dominant monoclinic phase domains coexist with a small fraction of tetragonal phase domains. Optical transmission and birefringence were significantly enhanced by a prior E-field poling. The Cauchy equations for ordinary n_o and extraordinary n_e refractive indices were determined between 0.45 and 1.4 μm. However, the phase-matching criterion for second-harmonic generation was not found. © *2005 American Institute of Physics*. [DOI: 10.1063/1.1862314]

I. INTRODUCTION

Recent developments on relaxor-based ferroelectrics $Pb(Mg_{1/3}Nb_{2/3})_{1-x}Ti_xO_3$ (PMNT) have demonstrated that high-quality crystals can be grown successfully and enhance piezoelectric performance radically compared with $Pb(Zr_{1-x}Ti_x)O_3$ (PZT) ceramics.[1] Physical properties of PMNT strongly depend on Ti content, external electric (E)-field strength, and crystallographic orientation.[2–7] The ultrahigh piezoelectric response has been theoretically attributed to polarization rotations between tetragonal (T) and rhombohedral (R) phases through intermediate monoclinic (M) or orthorhombic (O) symmetries.[8]

From synchrotron x-ray diffraction, an M_A-type M phase was observed in a (001)-cut PMNT35% crystal after a prior poling (E=43 kV/cm), but the unpoled and weakly poled samples exhibit an average R symmetry.[3] From field-induced domain observations at room temperature, $R \rightarrow M_A \rightarrow T_{001}$ and $R \rightarrow M_A \rightarrow T \rightarrow M_A \rightarrow R_{111}$ transition sequences were evidenced, respectively, in (001)-cut PMNT24% and (111)-cut PMNT33% as E field increases along oriented directions.[4,5] An M_C-type M phase was confirmed at 20 and 300 K by synchrotron x-ray diffraction for unpoled PMNTx% ceramics with $31 \leqslant x \leqslant 37$, in which the M phase was mixed with higher-symmetry phases, R, T, or O.[6] A field-induced $R \rightarrow O$ phase transition versus an M_B-type M phase was proposed for a (110)-cut PMNT30% crystal.[7] In poled PZT ceramic, an M phase was reported over a narrow composition range near the morphotropic phase boundary (MPB) and plays a key role in rotating the polarization from the $\langle 001 \rangle$ T phase to the $\langle 111 \rangle$ R phase.[9] Note that transitions of $R \leftrightarrow O$, $O \leftrightarrow T$, or $R \leftrightarrow T$ are of first order based on the Landau theory.[10]

Refractive indices of a (001)-cut PMNT38% crystal with a prior poling at E=10 kV/cm show a clear birefringence, but the phase-matching condition for second-harmonic generation was not found.[11] The optical transmission was also enhanced by a prior poling. With an assumption of an optically isotropic pseudocubic state, the refractive indices were determined at room temperature by spectroscopic ellipsometry for unpoled PMNTx% crystals with x=24, 30, 31, and 33.[12] It was found that refractive index increases with Ti content.

To enhance piezoelectric performance, a prior E-field poling process has usually been used before employing these materials in applications. However, how a prior E-field poling affects phase thermal stability and optical properties still remains unclear. In this study, temperature-dependent dielectric permittivity, domain structure, and hysteresis loop (polarization versus electric field) were investigated in a (001)-cut PMNT35% single crystal with and without a prior dc E-field poling. In addition, optical transmission and refractive indices were measured in a wide wavelength range.

II. EXPERIMENTAL PROCEDURE

The PMNT crystal was grown using a modified Bridgman method. The sample was cut perpendicular to a $\langle 001 \rangle$ direction. The Ti concentration (x) was determined by using the dielectric maximum temperature T_m (upon heating for f =10 kHz without a prior poling), i.e., $x=(T_m+10)/5$, where T is in °C.[13] For dielectric measurements, a variable-frequency Wayne–Kerr Precision Analyzer PMA3260A with four-lead connections was used to measure capacitance and

[a]Author to whom correspondence should be addressed; electronic mail: phys1008@mails.fju.edu.tw

0021-8979/2005/97(6)/064112/5/$22.50

resistance, and to obtain real ε' and imaginary ε'' parts of dielectric permittivity. A Janis CCS-450 closed cycle refrigerator was used with a Lakeshore Model 340 temperature controller. The temperature ramping rate was 1.5 K/min. Gold electrodes were deposited on sample surfaces by radio-frequency sputtering. Before any measurement described below, the sample was annealed above T_m. Two processes were used in the dielectric study. The first is called "zero-field heating" (ZFH), in which the data were taken upon heating without an E field or a prior poling. In the second process FR-ZFH, the sample was poled at room temperature with a dc E field, then cooled to 150 K without an E field before ZFH was performed. During the FR process, a dc E field was applied along the [001] direction. The remanent polarization (P_r) was also measured by using a Sawyer–Tower circuit at frequency of 46 Hz.

The domain structures were observed by using a Nikon E600POL polarizing microscope with a crossed polarizer/analyzer (P/A) pair. Transparent conductive films of indium tin oxide (ITO) were deposited on sample surfaces by radio-frequency sputtering. The experimental configuration for domain observation can be found in Ref. 4. The refractive indices were measured by using a Metricon Model 2010 Prism Coupler with three laser wavelengths, 0.473, 0.790, and 1.323 μm.

A brief review of principles for interpreting polarizing microscope photographs may be helpful. The propagation direction $\vec{k}$ of the polychromatic "white" light is along [001] for this work. Most of the information is obtained from observation of optical extinction, which occurs if both the following conditions are satisfied: (1) there must be no optical activity for the direction $\vec{k}$, (2) either $\vec{k}$ must lie along an optical axis, or if $\vec{k}$ is not along an optical axis, the incident $\vec{E}$ must lie along one of the two perpendicular axes in the plane perpendicular to $\vec{k}$ for which the optical-frequency permittivity is maximum or minimum. Uniaxial crystal structures, such as T and R phases, have optical axes and polarizations along $\langle 001\rangle$ and $\langle 111\rangle$, respectively. A clear mathematical analysis for the general extinction problem including biaxial symmetries such as O and M appears in Sommerfield[14] and Hartshorne and Stuart.[15]

Figure 1 shows the (001)-cut projection (with all four sides folded out) of relations among the various phases and corresponding polarizations for the primitive unit cell ($Z=1$) and double-size orthorhombic cell ($Z=2$). The squares indicate the directions of tetragonal polarization vectors **P**. The triangles indicate the directions for rhombohedral **P**'s. The circles indicate the directions for orthorhombic **P**'s. The solid, dash-dot, and dashed lines indicate the directions that polarizations can take for monoclinic cells based on the double-size ($Z=2$) orthorhombic cell. The dotted lines alternate between squares and circles, indicating directions that polarizations can take for monoclinic cells based on the simple ($Z=1$) cubic cell. Any polarization whose direction does not correspond to one of the three symbol types or four types of lines results from a triclinic cell. Domains that are optically inactive for $\vec{k}$ along [001] will have optical extinction for optical electric field along the radial and circumferential axes indicated by solid crossed lines inside the symbols. The solid lines between some symbols indicate no shift in optical extinction directions away from those in symbols connected by these lines. The lines for the remaining $Z=2$ (dashed and dash dot) and $Z=1$ (dotted) M polarization directions indicate shift in optical extinction direction away from radial and circumferential axes. The central "black" square indicates total extinction for any optical field direction for the [001] and [00$\bar{1}$] T domains. The M_C cell **P** lies between two adjacent T and O **P** vectors. The M_A cell has **P** between two adjacent T and R **P** vectors, whereas the M_B cell has **P** between two adjacent R and O **P** vectors. Accordingly, higher-symmetry phases (O, R, or T) with nearby polarization **P** directions are related by monoclinic phases. The details for using optical extinction to distinguish various phases in the (001)-cut sample can be found in Ref. 4.

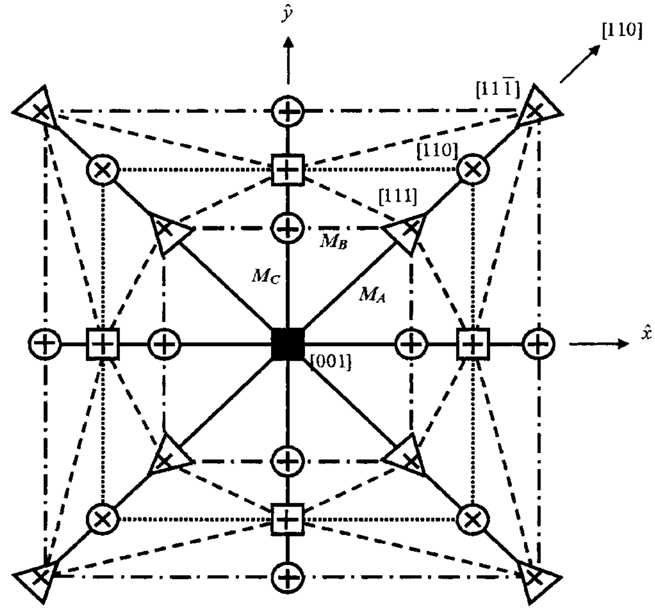

FIG. 1. Relation between the optical extinction orientations corresponding to the polarizations for various phases and domains projected on the (001) plane.

III. RESULTS AND DISCUSSION

Figure 2 shows the temperature- and frequency-dependent dielectric permittivities ε' and ε'' obtained from ZFH and FR-ZFH. The dielectric maximum temperature T_m is almost the same in ZFH and FR-ZFH. The smaller ε' in FR-ZFH is due to a poling effect which is expected to reduce the contribution of domain-wall motion. Instead of the gradual climb seen in the ZFH, ε' (FR-ZFH) exhibits a step-like decline in the region of 190–210 K associated with a weak frequency dispersion.

More complicated anomalies were observed in the imaginary part ε'', known as the dielectric absorption. In the ZFH, as given in the inset of Fig. 2(b), a clear frequency-dependent maximum and a weak shoulder (whose position is almost frequency independent, but not its amplitude) appear, respectively, in the regions of 120–180 K and 200–220 K, implying two different physical origins. The frequency-dependent behavior usually correlates to a relaxation pro-

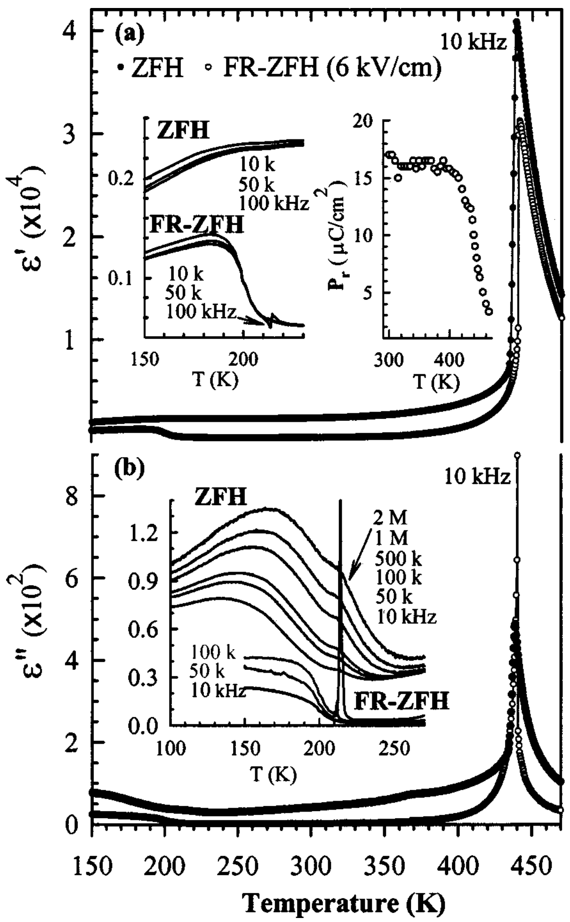

FIG. 2. Dielectric permittivities of ZFH and FR-ZFH (6 kV/cm) measured at f=10 kHz.

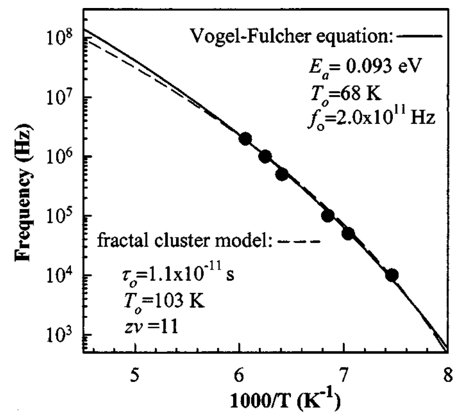

FIG. 3. Frequency vs 1000/T. T is the temperature corresponding to ε'' (ZFH) maximum in the region of 120–180 K. The solid and dashed lines are, respectively, fittings of Eqs. (1) and (2) with parameters given in the figure.

cess. After the FR (E=6 kV/cm), the frequency-dependent maximum seen in the ZFH (120–180 K) was obviously compressed, and the weak shoulder becomes a frequency-independent sharp peak at 212 K which exhibits stronger intensity at higher frequency. It indicates that the relaxation mechanism seen in the region of 120–180 K was suppressed after the FR, and a long-range percolation of polar clusters takes place near 212 K.

In a pure PMN crystal an extra dielectric peak was also observed at $T_c \sim 212$ K in a field-heating process, and was attributed to the percolating polar clusters due to the suppression of the random fields originating from compositional fluctuations at the B site.[16] Another important feature is that the imaginary part ε'' after a prior poling is much less than that without poling. For instance, the ratio of ε''(FR-ZFH)/ε''(ZFH) measured at room temperature is about 1/20. Low loss is an important criterion for high-power piezoelectric components.

What is the physical origin of the frequency-dependent maximum of dielectric absorption ε'' (ZFH) in the region of 120–180 K? Figure 3 shows a plot of measured frequency versus 1000/T and an exponential fitting (solid line) of the phenomenological Vogel–Fulcher equation commonly used in mixed systems;

$$f = f_o e^{-E_a/k_B(T-T_o)}, \tag{1}$$

where f is the measured frequency, f_o is a characteristic frequency (attempt frequency), and E_a is the activation energy for orientation of electric dipoles. T_o is the freezing temperature and T is the temperature corresponding to maximum ε'' (ZFH) in the region of 120–180 K. The fitting parameters are shown in Fig. 3. What is the significance of these parameters? First, the attempt frequency is in the usual range for lattice vibration. Second, T_o is the temperature at which all reorientation and coupling of clusters would cease. Third, E_a is the average of activation potential barriers for various clusters in this disordered system to reorient between adjacent variants. Compared with PMNT10% ceramic which has E_a=0.041 eV and T_o=291.5 K,[17] the higher activation energy in PMNT35% crystal implies a stronger correlation between polar clusters, which gives rise to a slower process to reach equilibrium in the system. Fitting the data to the Arrhenius law [T_o=0 in Eq. (1)] requires an unphysically high f_o.

Another approach to understand this relaxation process is the fractal cluster model,[18]

$$\tau = \tau_o \left(\frac{T}{T - T_o} \right)^{z\nu},$$

or

$$f = f_o \left(\frac{T}{T - T_o} \right)^{-z\nu}, \tag{2}$$

where $z\nu$ is called the dynamic exponent and T_o is the freezing temperature. τ is the critical relaxation time and $\tau_o = f_o^{-1}$ is the characteristic relaxation time. In this model the critical relaxation time τ and the collective cluster size s_ξ are related to the correlation length ξ by $\tau \sim \xi^z$ and $s_\xi = \xi^D$. D is the collective cluster fractal dimensionality. ξ diverges with temperature as $\xi \sim [T/(T-T_o)]^\nu$. The fitting (dashed line) and parameters of the fractal cluster model are given in Fig. 3. A similar dielectric phenomenon was seen in an as-grown (001)-cut PMNT32% crystal and was examined by the fractal cluster model with parameters, $z\nu$=11, T_o=43.3 K, and $\tau_o = 5.8 \times 10^{-10}$ s.[18] It was suggested that structural irregular

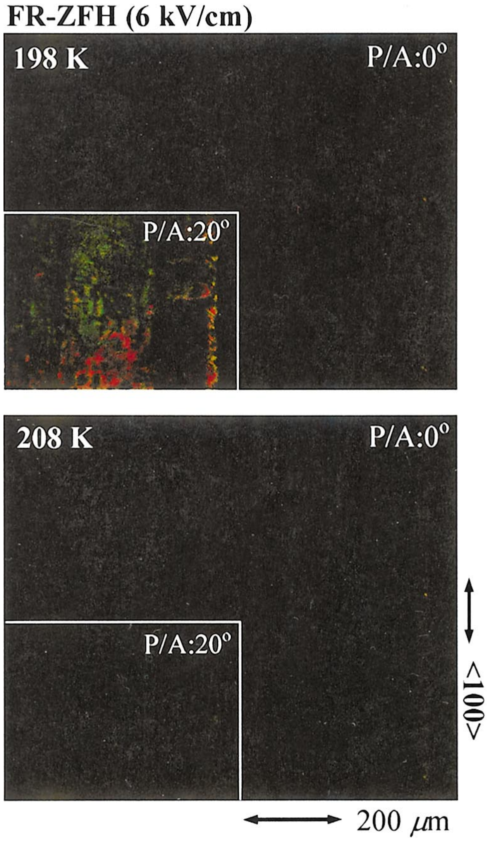

FIG. 4. (Color) Domain structures observed in the FR-ZFH at 198 and 208 K.

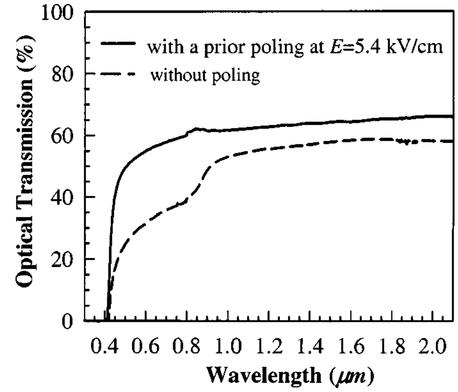

FIG. 6. Optical transmission without poling and with a prior poling at $E=5.4$ kV/cm.

ity plays a critical role in the dielectric absorption. This suggestion seems appropriate also for our system because the Arrhenius law does not apply, whereas the Vogel–Fulcher equation and fractal cluster model which apply to a system with structural irregularity give good fits with physically reasonable parameters.

ZFH domain structures observed after an E-field poling with $E=6$ kV/cm at room temperature, i.e., FR-ZFH (6 kV/cm), are shown in Fig. 4 for 198 and 208 K. Angles of the P/A pair presented in Fig. 4 are with regard to the ⟨001⟩ direction. Below 198 K the domain matrix exhibits extinction from 0° to 10°, but near 208 K the crystal shows extinction from 0° to 20°. A similar phenomenon was seen in the pure ZFH domain observation, but not as apparent as the FR-ZFH. When observing the (001)-cut sample along [001] between a crossed P/A pair, as shown in Fig. 1, T and M_C-type M phase domains have extinction at 0° with regard to [100]. The R phase domains show optical extinction at 45°. The wide extinction range (0°–20°) reveals that domains polarizations are in the vicinity of the [001] T polar direction and most likely are M phase. At $E=9$ kV/cm, the crystal mostly reaches total extinction, indicating a single domain poled along [001].

Without a prior poling ($E=0$), as shown in Fig. 5, the ⟨002⟩ x-ray diffraction exhibits four major peaks as indicated by dashed lines with number labels (1–4). Based on the cubic structure, lattice parameters calculated from peak positions are given in Fig. 5. According to Ref. 6, beside an M phase a dominant T phase was found in the unpoled PMNT35% ceramic with lattice parameters $a=4.000$ Å and

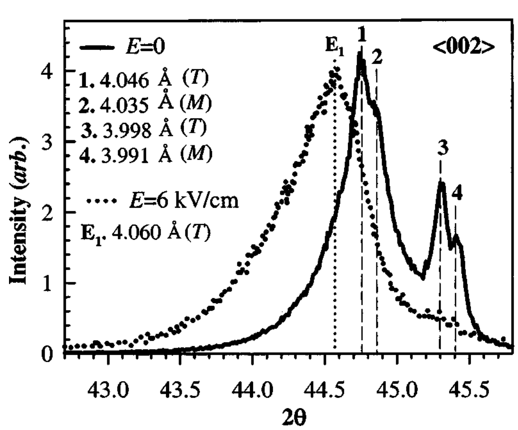

FIG. 5. ⟨002⟩ x-ray diffraction spectra with and without a prior E-field poling along [001]. The calculated lattice parameters and possible symmetries are given in the figure. T and M represent, respectively, tetragonal and monoclinic symmetries.

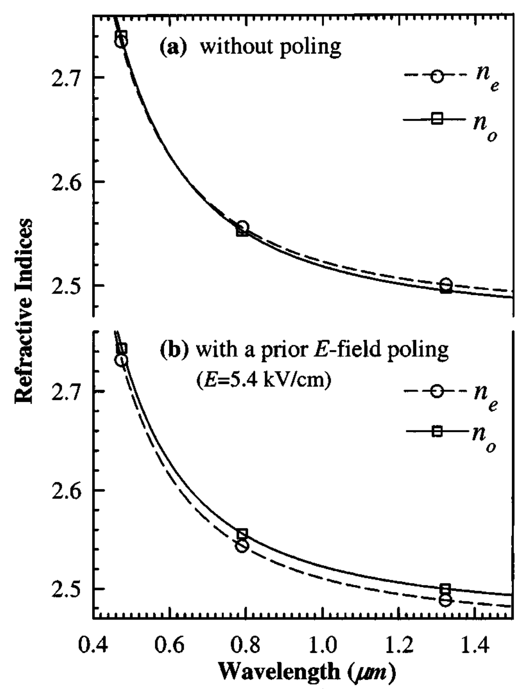

FIG. 7. Refractive indices measured at room temperature. The curves are fittings of the Cauchy equation with parameters given in Table I.

TABLE I. The Cauchy equations of $n_o(\lambda)$ and $n_e(\lambda)$ measured at room temperature without poling ($E=0$) and with a prior dc E-field poling at $E=5.4$ kV/cm, where λ is in μm.

$E=0$	$n_o(\lambda)=2.4649+(0.0512/\lambda^2)+(0.0023/\lambda^4)$,	$n_e(\lambda)=2.4720+(0.0488/\lambda^2)+(0.0022/\lambda^4)$
$E=5.4$ kV/cm	$n_o(\lambda)=2.4716+(0.0483/\lambda^2)+(0.0029/\lambda^4)$,	$n_e(\lambda)=2.4606+(0.0467/\lambda^2)+(0.0032/\lambda^4)$

$c=4.044$ Å. Thus, diffraction peaks (1–4) most likely correlate to symmetries of T and M phases. After the FR ($E=6$ kV/cm), only a strong diffraction peak (as indicated by the dashed line and E_1) was observed with a weak shoulder at $2\theta\cong 45.3°$. The calculated lattice parameter of E_1 peak is about 4.060 Å and possibly correlates to lattice parameter c of T symmetry. Based on the above evidence, a long-range $M(T)\rightarrow T(M)$ transformation likely takes place near 210 K after the FR. $M(T)$ represents that dominant M phase domains coexist with a smaller fraction of T phase domains. The crystal becomes cubic phase near 440 K, where the P_r exhibits a rapid decline, as seen in the inset of Fig. 2(a).

Wavelength-dependent optical transmission from 0.3 to 2.1 μm, given in Fig. 6 shows little absorption before reaching the cut-off wavelength $\lambda\cong 0.4$ μm, which is the same with and without a prior E-field poling. It shows that a prior poling process can enhance the optical transmission by about 20%, likely due to reduction of internal reflection by domain walls and strains. The transmission cutoff at $\lambda\cong 0.4$ μm implies an average electronic energy gap of about 3.0 eV. The transmission of PMNT thin films goes to zero at $\lambda\cong 0.35$ μm.[19]

Figure 7 shows ordinary n_o and extraordinary n_e refractive indices measured at room temperature without poling ($E=0$) and with a prior poling ($E=5.4$ kV/cm). The refractive indices are higher than those obtained from PMNT35% thin films[20] and from the nonlinear optical crystal $RbTiOAsO_4$ (RTA).[21] In the prior poling process, the crystal was poled at room temperature along a ⟨010⟩ direction which is the optical axis of the uniaxial tetragonal structure. Without a prior poling, the crystal shows very small birefringence $|n_o-n_e|$ which is less than 0.004 at $\lambda=0.790$ μm. This phenomenon reveals that the tetragonal distortion is so small that the average symmetry can be considered as optically isotropic. Interestingly, after a prior poling at $E=5.4$ kV/cm, the crystal shows a noticeable "negative" uniaxial birefringence and $|n_o-n_e|$ is about 0.0129 at $\lambda=0.790$ μm. It was found that the birefringence does not increase noticeably even with a higher poling field ($E>5.4$ kV/cm). For instance, after a prior poling at $E=12$ kV/cm, the refractive indices are $n_o=2.5025$ and $n_e=2.4908$ at $\lambda=1.323$ μm, and $n_o=2.5583$ and $n_e=2.5466$ at $\lambda=0.790$ μm. By fitting refractive indices measured from three laser wavelengths, the Cauchy equations of n_o and n_e were obtained without and with a prior poling ($E=5.4$ kV/cm), as given in Table I. The calculation of phase-matching angle[22] for second-harmonic generation shows that the phase-matching condition does not exist.

IV. CONCLUSIONS

This work reveals phase thermal stability of (001)-cut PMNT35% crystal with and without a prior dc E-field application along [001]. Without an E-field poling, a frequency-dependent maximum was observed in the ZFH dielectric absorption in the region of 120–180 K. This dispersion phenomenon can be described by the Vogel–Fulcher equation and fractal cluster model, and likely associated with structural irregularity in the domain matrix. After a dc E field poling, this relaxation behavior was suppressed and a long-range percolation associated with an $M(T)\rightarrow T(M)$ transition takes place near 212 K, which is signified by a sharp frequency-independent loss peak. Both optical transmission and birefringence were significantly enhanced by a prior E-field poling, likely due to a formation of a long-range ordered state. The Cauchy equations of refractive indices n_o and n_e were obtained, but the phase-matching condition for second-harmonic generation was not found in this work.

ACKNOWLEDGMENTS

The authors would like to thank Dr. Pengdi Han (H.C. Materials Corp.) for crystals and W.-T. Shu (Physics Department of Fu Jen University) for experimental help. This work was supported by DoD EPSCoR Grant No. N00014-02-1-0657 and NSC Grant Nos. 92-2112-M-030-007 and 93-2112-M-030-001.

[1] P. Han, *Abstract Book of the Fundamental Physics of Ferroelectrics* (Williamsburg, Virginia, 2004), pp. 72–73.
[2] T. R. Shrout, Z. P. Chang, N. Kim, and S. Markgraf, Ferroelectr., Lett. Sect. **12**, 63 (1990).
[3] Z.-G. Ye, B. Noheda, M. Dong, D. Cox, and G. Shirane, Phys. Rev. B **64**, 184114 (2001).
[4] R. R. Chien, V. H. Schmidt, C.-S. Tu, L.-W. Hung, and H. Luo, Phys. Rev. B **69**, 172101 (2004).
[5] C.-S. Tu, I.-C. Shih, V. H. Schmidt, and R. Chien, Appl. Phys. Lett. **83**, 1833 (2003).
[6] B. Noheda, D. E. Cox, G. Shirane, J. Gao, and Z.-G. Ye, Phys. Rev. B **66**, 054104 (2002).
[7] D. Viehland and J. F. Li, J. Appl. Phys. **92**, 7690 (2002).
[8] H. Fu and R. E. Cohen, Nature (London) **403**, 281 (2000).
[9] R. Guo, L. E. Cross, S.-E. Park, B. Noheda, D. E. Cox, and G. Shirane, Phys. Rev. Lett. **84**, 5423 (2000).
[10] D. Vanderbilt and M. H. Cohen, Phys. Rev. B **63**, 094108 (2001).
[11] X. Wan, H. Xu, T. He, D. Lin, and H. Luo, J. Appl. Phys. **93**, 4766 (2003).
[12] X. Wan, H. L. W. Chan, C. L. Choy, Z. Zhao, and H. Luo, J. Appl. Phys. **96**, 1387 (2004).
[13] Z. Feng, H. Luo, Y. Guo, T. He, and H. Xu, Solid State Commun. **126**, 347 (2003).
[14] A. Sommerfeld, *Optics* (Academic, New York, 1964), pp. 129–139.
[15] N. H. Hartshorne and A. Stuart, *Crystals and the Polarising Microscope* (E. Arnold Ltd., London, 1970).
[16] V. Westphal and W. Kleemann, Phys. Rev. Lett. **68**, 847 (1992).
[17] D. Viehland, S. J. Jang, and L. E. Cross, J. Appl. Phys. **68**, 2916 (1990).
[18] S. Priya, D. Viehland, and K. Uchino, Appl. Phys. Lett. **80**, 4217 (2002).
[19] K. Y. Chan, W. S. Tsang, C. L. Mak, and K. H. Wong, Phys. Rev. B **69**, 144111 (2004).
[20] W. S. Tsang, K. Y. Chan, C. L. Mak, and K. H. Wong, Appl. Phys. Lett. **83**, 1599 (2003).
[21] C.-S. Tu, R. S. Katiyar, V. H. Schmidt, R. Guo, and A. S. Bhalla, Phys. Rev. B **59**, 251 (1999).
[22] A. Yariv, *Optical Electronics* (Saunders College Publishing, San Francisco, 1991), pp. 270–274.